

## Preparation and Characterization of All Para-Position Polysulfonamide Fiber

Humin Li, Yin Zhu, Bing Xu, Chengxun Wu, Jiongxin Zhao, Mingxin Dai

State Key Laboratory for Modification of Chemical Fibers and Polymer Materials, College of Material Science and Engineering, Donghua University, Shanghai 201620, People's Republic of China

Correspondence to: J. X. Zhao (E-mail: zjxin@dhu.edu.cn)

**ABSTRACT:** Poly(4,4'-diphenylsulfone terephthalamide) referred to as all para-position polysulfonamide (all para-position PSA) is a special kind of PSAs, copolymers of 3,3'-diaminodiphenylsulfone, 4,4'-diaminodiphenylsulfone, and terephthaloyl chloride. However, with the increasing para-structure content in the PSAs, the PSA shows very poor solubility in common amide-type polar aprotic solvents and cannot be used for wet spinning. In this article, it was found that all para-position PSA can be easily dissolved in N,N-Dimethylacetamide (DMAc)/LiCl system, and then the all para-position PSA fiber was prepared for the first time by wet spinning. The properties of all para-position PSA pulps and fibers were investigated via Fourier transform infrared spectroscopy (FTIR), nuclear magnetic resonance (NMR), scanning electron microscopy, thermal gravimetric analysis, dynamical mechanical analysis, X-ray diffraction (XRD), and tensile strength testing. The tensile strength, elongation at break, and crystallinity of the resulting fiber were 4.4 cN/dtex, 15.9%, and 33.53%, respectively. The results indicated that all para-position PSA fiber was a high-temperature resistance fiber with better mechanical properties than common PSA fiber. The improved tensile strength of the fiber will expand its applications and may take place of Nomex in certain fields and become a new generation of flame retardant and high-temperature resistant material. © 2012 Wiley Periodicals, Inc. *J. Appl. Polym. Sci.* 000: 000–000, 2012

**KEYWORDS:** all para-position polysulfonamide fiber; thermal stability; DMAc/LiCl system; wet spinning

Received 4 January 2012; accepted 14 April 2012; published online

DOI: 10.1002/app.37896

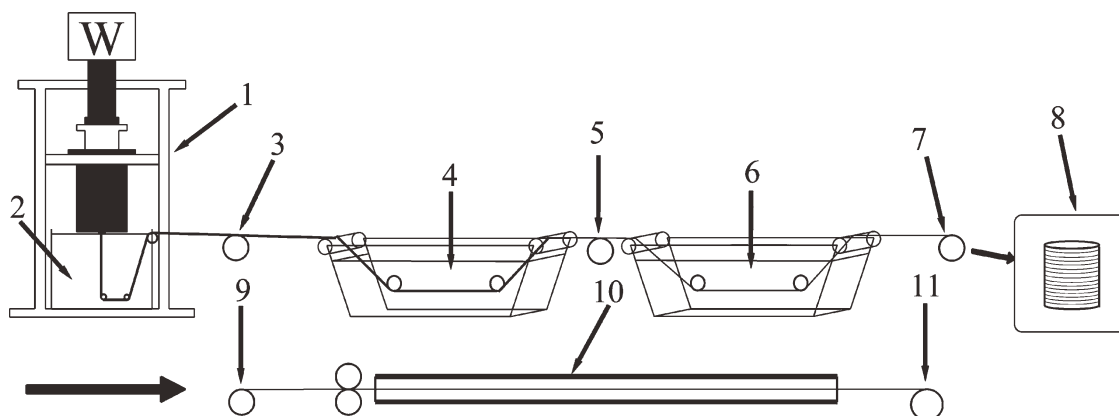
### INTRODUCTION

Polysulfonamides (PSAs) fiber is a high-temperature resistance fiber under China's independent intellectual property rights.<sup>1,2</sup> It was first developed by Shanghai Textile Research Institute and Shanghai Synthetic Fiber Research Institute in 1974, which provided a kind of synthetic fiber of the 250°C temperature resistant grades. PSA fiber belongs to aromatic polyamide polymer materials. Due to the existence of the conjugated aromatic rings and the additional sulfone ( $-\text{SO}_2-$ ) group structure in its molecular main chain, the PSA fiber with such molecular structure cannot be easily destroyed at high temperature, it performs better in thermal stability than aramid fiber.<sup>3,4</sup> Compared with other high-performance products, PSA fiber has excellent mechanical properties, high-temperature resistance performance, flame-retardant properties, and easy dyeing properties. The limiting oxygen index of PSA fiber may reach up to 33, whereas that of Nomex is 29.<sup>5,6</sup> These features enabled PSA fiber to have applications in the high-temperature filtration field. Besides, PSA fiber can be widely used as insulation materials, protective

textiles, composite materials, membrane materials, and so on.<sup>4</sup> As early as 1980s, PSA, also as an excellent membrane material, has been deeply studied and widely used for the preparation of reverse osmosis, ultrafiltration, and microfiltration membranes.<sup>7–10</sup> Recently, PSA fiber has emerged as a new reinforcing material with the advantages of low cost and rich resources.<sup>3</sup> Jia et al.<sup>11–13</sup> have investigated the ablation and thermal properties of ethylene-propylene-diene elastomer composites reinforced with PSA short fiber.

However, the strength of common PSA fiber has still limited its application area. Improving the strength of PSA fiber is emergent. To address this problem, Liu et al.<sup>14</sup> introduced rigid aramid linkages and aryl ether into the main chain of the PSA, and the PSA copolymers exhibited enhanced tensile strength and still maintained the thermal stability. And Yu et al.<sup>15</sup> studied the influence of spinning solution properties on the coagulation process of PSA fiber and obtained the most important factors related to enhancing the mechanical properties of the final PSA fiber. Chemically, the common PSA is a copolymer

© 2012 Wiley Periodicals, Inc.



**Scheme 1.** Schematic flow chart of spinning all para-position PSA fiber. 1, all para-position PSA solution; 2, coagulation bath; 3, 5, 7, 9, and 11 rollers; 4, second coagulation bath; 6, wash bath; 8, oven for drying; 10, hot tube.

synthesized by 3,3'-diaminodiphenylsulfone (3,3'-DDS), 4,4'-diaminodiphenylsulfone (4,4'-DDS), and terephthaloyl chloride (TPC). The melting temperature of PSA lies above the decomposition temperature, accordingly, the PSA should only be transformed to solution first and then the wet-spinning technique rather than melt spinning could be adopted for fiber preparation. In the earlier research, some articles also showed the properties of the PSA copolymers varies with the different component ratios of 4,4'-DDS to 3,3'-DDS: higher ratio of 3,3'-DDS component in the copolymer was related to better solubility, and higher ratio of 4,4'-DDS in the copolymer was related to higher elastic modulus, stronger tensile strength, and poorer solubility.<sup>16</sup> Poly(4,4'-diphenylsulfone terephthalamide) referred to as all para-position PSA here means that it was synthesized only by 4,4'-DDS and TPC and hence was expected to have best mechanical properties. However, the poor solubility of all para-position PSA in common amide-type polar aprotic solvents still makes it very difficult to prepare spinning solution.

In this study, we aimed to obtain all para-position PSA fiber with better mechanical properties, and for the first time, we found that all para-position PSA could be well dissolved in DMAc/LiCl system and that the solution could be well spun into fiber via wet-spinning technique.

## EXPERIMENTAL

### Materials

All para-position PSA with inherent viscosity of 0.62 dL/g was supplied by Shanghai Institute of Organic Chemistry, Chinese Academy of Sciences, Shanghai, China as our cooperator. LiCl and *N,N*-dimethylacetamide were purchased from Beijing Chemicals, Beijing, China and used without any further purification.

### Synthesis of the Polymer

4,4'-DDS (40.22 g) and 500 mL of DMAc were added into a 1000 mL three-necked round-bottom flask equipped with a mechanical stirrer and a nitrogen gas inlet, and the mixture was stirred to form homogenous solution and cooled to 0°C in ice-salt bath. And then 32.89 g of TPC was added in batches maintaining the reaction temperature below 20°C. Solution was then stirred for 1 h at 0°C, then 9.084 g of CaO was added into the solution at room temperature to neutralize HCl, which was produced during the reaction, and stirring was continued for additional 1 h at

room temperature. The resulting mixture was poured into water, and the polymer precipitate was filtered off, washed thoroughly with hot and cold water, extracted with water for 24 h in a Soxhlet extractor, and vacuum dried over P<sub>2</sub>O<sub>5</sub> at 110°C.

### Preparation of All Para-Position PSA Fiber

The spinning apparatus is illustrated in Scheme 1. All para-position PSA fiber was prepared via using a wet-spinning process. Spinning solution of 24 wt % all para-position PSA dissolved in the compound solvent of 2 wt % LiCl/DMAc was used to prepare the fiber. This all para-position PSA spinning solution was stored in a heated metal block and additionally filtrated with metal mesh sieve and degassed at 60°C there. The spinning solution was extruded as filaments at an extrusion rate of 4 m/min via a 6-pore spinneret into the coagulation bath at 60°C, the pore diameter was 0.1 mm. The coagulation bath was consisted of DMAc and water (60 wt % DMAc/40 wt % water) at 10°C. The as-spun fibers were then drawn between the two drawing rollers with a draw ratio of 2 in the second coagulation bath, containing 40 wt % DMAc/60 wt % water at 60°C. The drawn fibers were washed with hot water immediately and then dried in an oven at 160°C for 2 h. At last, the fibers were drawn in a hot tube with a draw ratio of 3 at 350°C.

### Characterization

FTIR spectra were recorded on (NEXUS-670, Nicolet) spectrometer at ambient temperature. The test specimens were prepared via KBr pellet method.

<sup>1</sup>H- and <sup>13</sup>C-NMR spectra were recorded on a Bruker Avance 400 spectrometer operating at 400 MHz (<sup>1</sup>H) and 100 MHz (<sup>13</sup>C), respectively, using deuterated dimethylsulfoxide as solvent and tetramethylsilane (TMS) as the internal standard.

The morphology and microstructure of the as-spun and finished fibers were characterized by a scanning electron microscope (SEM, S-3000N, Hitachi, Japan). For cross section observation, the as-spun fibers were fractured in liquid nitrogen and perpendicularly pasted on a sample-carrier, and then the samples were sputtered with gold prior to observation.

Oxygen index methods are widely used to measure and to represent the flammability and the effectiveness of fire retardants of

**Table I.** Properties of PSA Fibers, Nomex, and All Para-Position PSA Fibers

	PSA fibers	Nomex	All para-position PSA fibers
Tensile strength (cN/dtex)	2.4	4.4–6.3	4.4
Initial modulus (cN/dtex)	35	58.4–89.5	48
Density (g/cm <sup>3</sup> )	1.416	1.38	1.425
Water uptake (%), at 65% RH	6.28	5.2	5.92
Crystallinity	Low (15.83%)	High (68–95%)	Low (33.53%)
Glass transition temperature (°C)	257	275	372
Melting temperature (°C)	None	None	None
Flammability (L.O.I.)	33	29	33
Decomposition temperature in N <sub>2</sub> (°C)	400–425	400–430	400
Thermal shrinkage rate (%)			
Boiling water	0.5–1.0	3.0	0.72
Air at 300°C	2.0	8.0	1.55

polymers. The limiting oxygen index value of all para-position PSA was measured via using an oxygen index testing apparatus (FAA, ATS FAAR, Italy) with sheet dimensions of 130 × 6.5 × 3 mm<sup>3</sup>, according to ASTM D2863-97. The results are listed in Table I.

The thermal degradation of samples was measured using a thermal gravimetric analyzer (TGA, 209F1Iris, Netzsch) from 30 to 900°C at a heating rate of 10°C/min under air and nitrogen atmosphere, respectively.

The dynamical mechanical analysis (DMA) of fiber samples was carried out using a Q800 DMA instrument (TA, America) with a heating rate of 5°C min<sup>-1</sup> from 50 to 440°C.

Wide-angle X-ray diffraction (WAXD) analysis of all para-position PSA pulps and fibers was carried out via using an X-ray diffractometer (D/MAX-2550, Rigaku Denki, Japan) by a reflection method using a CuK $\alpha$  radiation at 40 kV and 30 mA. The diffraction angle ranged from 5 to 60°.

The mechanical properties of the fibers were measured using a tensile tester (LLY-06B, Laizhou Electron Instrument, China) according to GB/T method 14335-2008. The gauge length and crosshead speed for the tensile tests were 10 mm and 10 mm/min, respectively. For tensile tests, at least 10 filaments were tested in each case.

## RESULTS AND DISCUSSION

### Fourier Transform Infrared Spectral Analysis

The molecular structure of all para-position PSA was confirmed by FTIR and NMR spectroscopy, and the results were not entirely consistent with prior research.<sup>17</sup> A typical FTIR spectrum is shown in Figure 1. The FTIR spectrum of all para-position PSA exhibited the characteristic absorption bands of polyamides at 3200–3450 cm<sup>-1</sup> (N–H stretching), 1654 cm<sup>-1</sup> (C=O stretching), 1500–1524 cm<sup>-1</sup> (combined N–H bending and C–N stretching (amide-II band, interaction between –N–H deformation and –C–N stretching, strong band)). Bands attributed to disubstituted benzene appeared around 824 cm<sup>-1</sup>. Also, the FTIR spectrum displayed absorption peaks at 1138

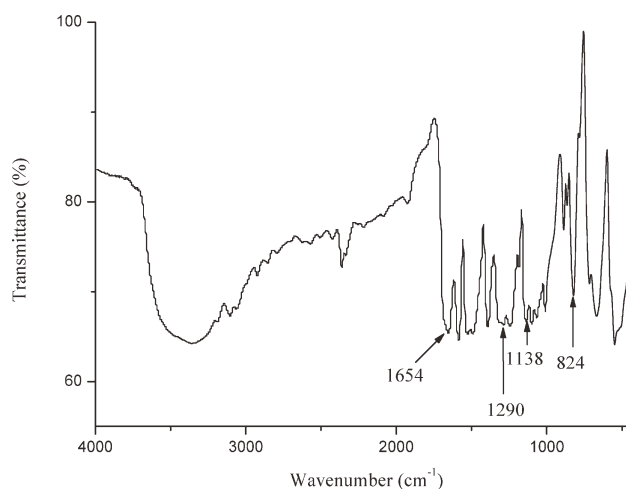
and 1290 cm<sup>-1</sup>, associated with asymmetric and symmetric –SO<sub>2</sub>– stretching, respectively.

### Nuclear Magnetic Resonance Analysis

<sup>1</sup>H- and <sup>13</sup>C-NMR were used to identify the structure of all para-position PSA. Figure 2 illustrates the <sup>1</sup>H- and <sup>13</sup>C-NMR spectra of PSA in dimethylsulfoxide (DMSO)-*d*<sub>6</sub> solution and the assignments to all carbons and protons. According to the empirical equations  $\delta_H = 7.27 - \sum S$  (where  $\delta$  is the chemical shift, and  $S$  is the influence of substituent group to the aromatic protons chemical shift) and  $\delta_C = 128.5 + \sum Z_i^{18}$  (where  $Z_i$  is the influence of substituent group to the aromatic carbons chemical shift), the  $\delta$  of all the aromatic protons and carbons can be estimated. It can be clearly seen that all the carbons and protons are in good agreement with the expected or proposed structure.

As it can be seen, in the <sup>1</sup>H-NMR, the absorption peak at 10.8 ppm was assigned to the N–H protons, and the absorption peaks appearing in the region of 7.9–8.2 ppm were assigned to the aromatic protons.

Also, the <sup>13</sup>C-NMR spectrum of all para-position PSA shows seven signals attributed to seven kinds of carbons of the

**Figure 1.** FTIR spectrum of all para-position PSA.

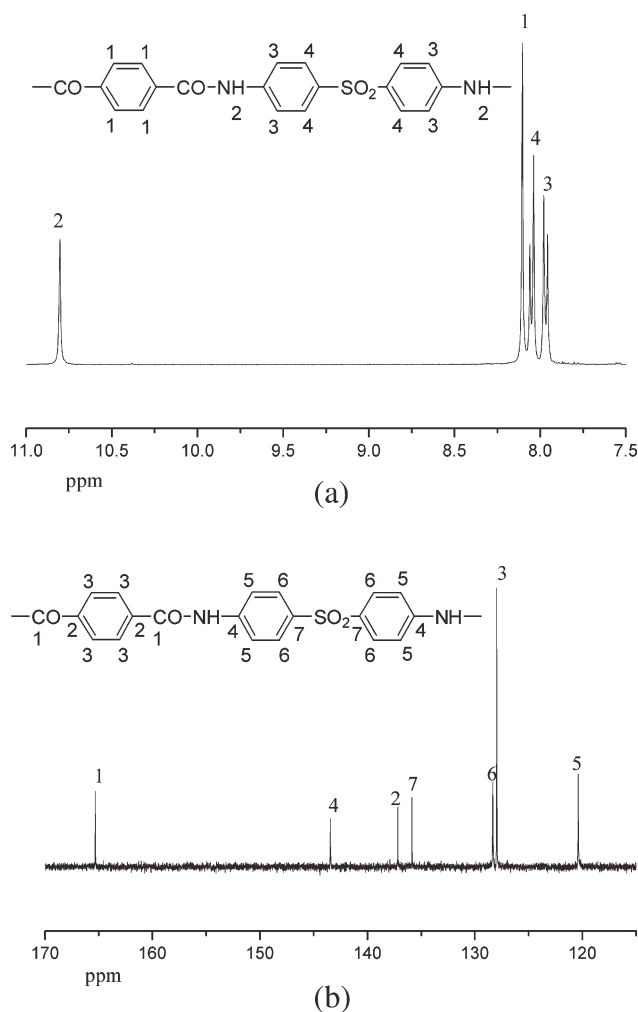


**Figure 2.** (a) The <sup>1</sup>H-NMR spectrum of all para-position PSA. (b) The <sup>13</sup>C-NMR spectrum of all para-position PSA.

structure. The absorption peak at 165 ppm was assigned to the carbons of  $\text{—C=O—}$ , and the absorption signals of aromatic carbons appear in the range of 120–145 ppm.

### Scanning Electron Microscopy

Figure 3(A,B) shows the cross section and surface morphology of the all para-position PSA as-spun fibers. Choosing of suitable spinning condition and coagulation condition was a complex problem, both conditions played important roles in determining the fiber properties. Normally, a higher DMAc concentration (related to water) of the solvent in the coagulation bath and a reduced coagulation temperature lead to lower coagulation rates and thus result in improved mechanical properties of the fiber. And commercially, PSA is often wet spun at low temperature in the range of 10–15°C to reduce the number of large voids produced in the as-spun fiber structure. In our study, the fibers cannot be formed or well coagulated when the DMAc concentration in the coagulation bath greater than 70%. Therefore, DMAc concentration (related to water) in the coagulation bath chosen is 60%. As it can be seen from Figure 3(A), under such still rather high-DMAc concentration in the coagulation bath, only sponge-like structure was obtained. Furthermore, under

such situation, the cross-sectional shape of the fiber was circular, and no skin-core morphology is visible. Many studies on the formation of macrovoids, sponge-like, finger-like, or macrovoid-free structure in phase-inversion processes can be found in the literature.<sup>19–22</sup> The result here indicated that the coagulation condition of 60 wt % DMAc/40 wt % water was excellent for the formation of the fiber. And the loose structure of the cross section was due to a certain extent of swelling of the fiber.

There was a small amount of pore on the surface of the as-spun fibers [Figure 3(B)], the pore size was about 1.5 μm, the formation mechanism of these pores was not very clear yet, but it must be a result of the coupled dual-diffusion of solvent and nonsolvent during the phase separation of the all para-position PSA spinning solution and also is a result of the contemporaneous effects of multiple spinning parameters.

The surface SEM photographs of finished fibers are shown in Figure 3(C). As it can be seen, after drawn via second coagulation bath and a hot tube, the final fiber with its diameter decreased appeared to have rough surface structure with irregular stripes. These were formed during drawing by the depression of voids in the fibers, such a phenomenon was common when fibers were elongated during formation.

### Thermogravimetric Analysis

Figure 4 shows TGA curves of the polymer in N<sub>2</sub> and air atmosphere. It can be seen that the all para-position PSA almost did not loss weight below 400°C in nitrogen and air, implying that no thermal decomposition occurred. The results indicated that the all para-position PSA exhibited almost the same initial decomposition temperature as that of Nomex.<sup>5,6</sup> The temperature of 10% weight loss was recorded at 477°C in air. It left about 3.4% residual weight in air and more than 40% residual weight in nitrogen at 900°C.

### Dynamic Mechanical Analysis

For a further insight into the behavior of all para-position PSA, dynamic mechanical analysis was performed to evaluate the glass transition temperature ( $T_g$ ) of the fiber, which is more sensitive to the changes occurring in  $T_g$  than the DSC method. The results are presented in Figure 5. The figure displays the dependence of storage modulus  $E'$ , loss modulus  $E''$  and damping factor ( $\tan \delta$ ) upon temperature at a fixed frequency of 1 Hz. As seen in the figure,  $E'$  and  $E''$  changed slowly with increasing the temperature before 300°C.  $E'$  showed only one-step decrease in the temperature range 300–380°C, and  $E''$  showed a sharp peak near 363°C, indicating occurrence of just one physical transition in the all para-position PSA fiber, corresponding to the glass transition region of the material. From the curve of  $E'$ , we could get two tangents, the intersection of two tangents could be assumed as the glass transition temperature (349°C). The temperature correspondent to the  $\tan \delta$  peak was taken as the glass transition temperature ( $T_g$ ) of the all para-position PSA fiber in this article. There was a single, sharp, and symmetrical relaxation peak for the material, and the  $T_g$  of the all para-position PSA was 372°C, which was much higher than that of Nomex ( $T_g = 275^\circ\text{C}$ ).<sup>5,6</sup> The results confirmed that, when related to mechanical properties, all para-position PSA could be used at or below 250°C for a long term.

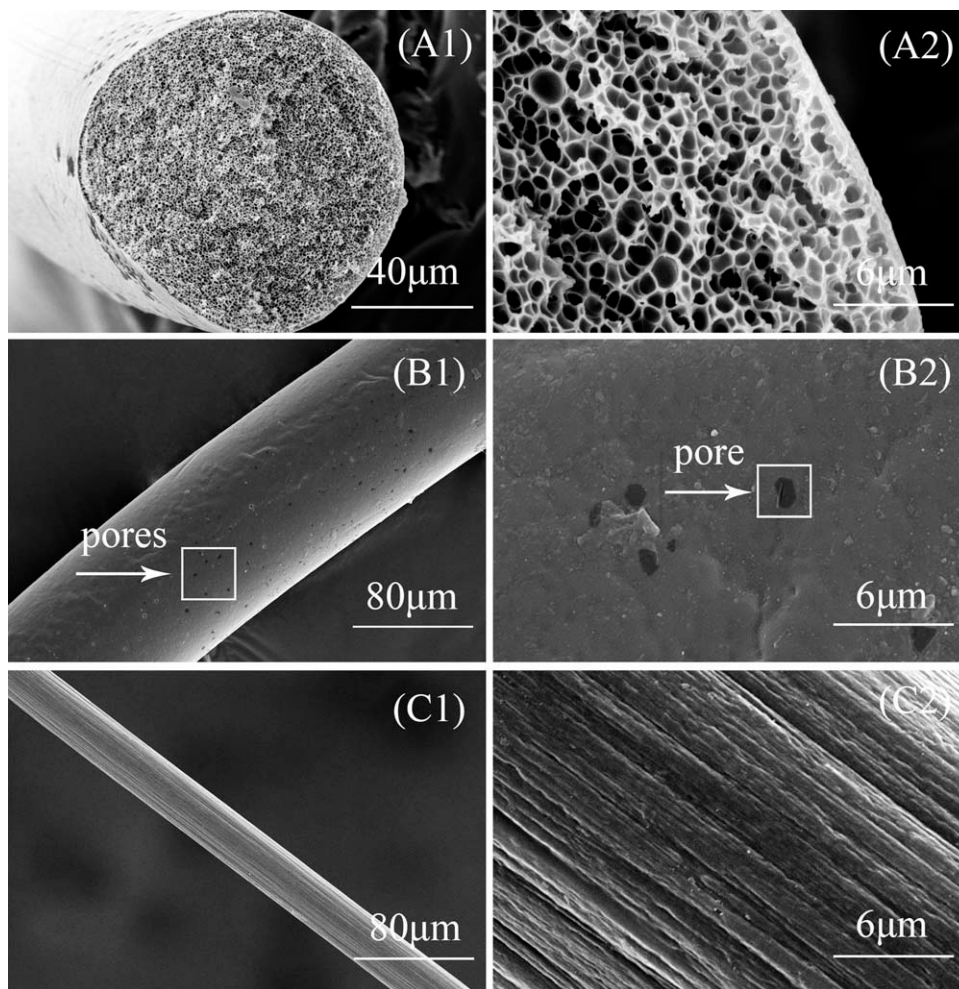


**Figure 3.** SEM photographs of the cross section and surface of the all para-position PSA as-spun fibers and finished fibers. Cross section of as-spun fibers: A1 and A2; surface of as-spun fibers: B1 and B2; surface of finished fibers: C1 and C2.

#### X-Ray Diffraction of All Para-Position PSA Pulps and Fibers

The WAXD patterns of all para-position PSA pulps and fibers are shown in Figure 6. Figure 6(a) indicated that the crystallin-

ity of the all para-position PSA pulps was very low. After being spun and drawn, the peak at  $2\theta = 16.1^\circ$  shows a significant decrease in the width at half maximum. This was an indication of an increase in the crystallinity of all para-position PSA fibers. According to the Hermans and Weidinger's equation,

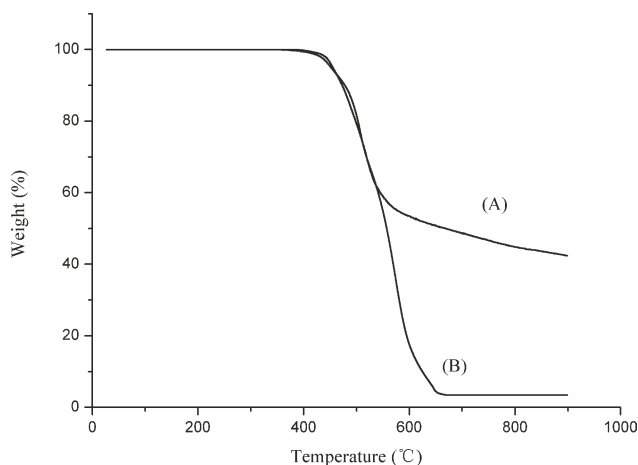


**Figure 4.** TGA curves of all para-position PSA in nitrogen (A) and air (B).

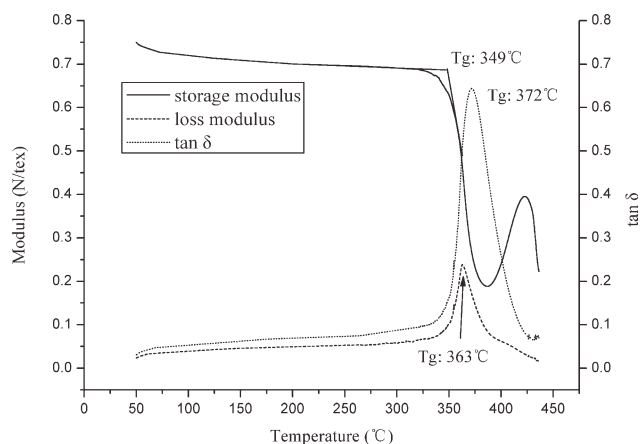


**Figure 5.** Dynamic mechanical analysis of all para-position PSA fiber.

$X_c = \frac{S_c}{S_c + S_a}$  (where  $S_c$  and  $S_a$  are the diffraction area of crystalline and amorphous region, respectively). We can determine the crystallinity ( $X_c$ ) of PSA pulps and fibers. The crystallinity of all para-position PSA pulps increased from 20.87 to 33.53% after being spun.

From the Scherrer's equation,<sup>25</sup> we can estimate the crystallite size ( $D$ ) of all para-position PSA pulps and fibers.

$$D = \frac{k\lambda}{\beta \cos \theta}$$

where  $D$  is crystallite size,  $\lambda$  is wavelength of CuK $\alpha$  radiation ( $\lambda = 1.54 \text{ \AA}$ ),  $\theta$  is Bragg's angle,  $\beta$  is width at half maximum in radians, and  $k$  is a constant taken as 1 here.<sup>26</sup> The crystallite size of the polymer increased from 2.59 to 4.85 nm due to spinning and drawing.

Figure 6(b) shows X-ray azimuthal scan for measuring the crystalline orientation of the all para-position PSA fiber. According to the empirical equation  $R = [(360 - \sum H_i)/360] \times 100\%$ <sup>25</sup>

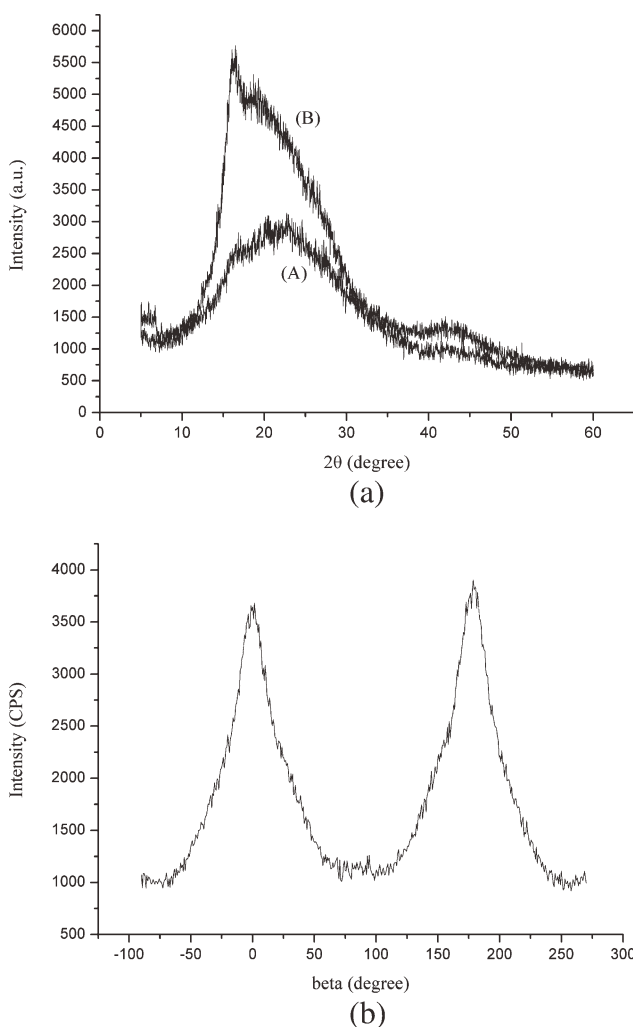


**Figure 6.** (a) XRD patterns of all para-position PSA pulps (A) and fibers (B). (b) X-ray azimuthal scan for measuring the crystalline orientation of the all para-position PSA fibers.

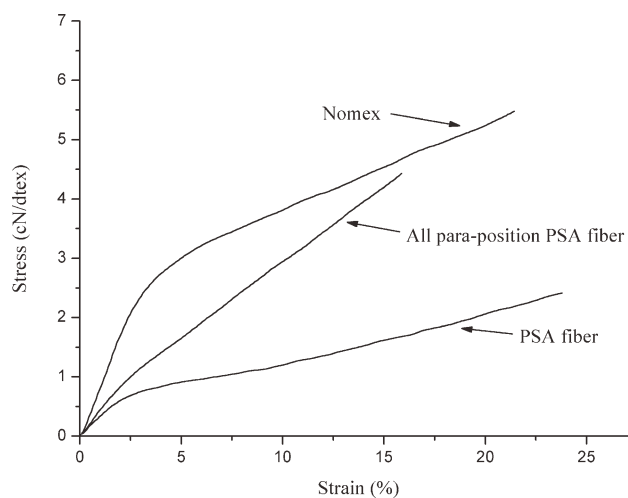


**Figure 7.** Stress-strain curves of Nomex, PSA fiber, and all para-position PSA fiber.

(where  $H_i$  is width at half maximum in degree of peak  $i$ ), the crystalline orientation factor of the final fiber was 71.3%.

#### Mechanical Properties of All Para-Position PSA Fibers

The stress-strain curves of Nomex, PSA fibers, and all para-position PSA fibers are shown in Figure 7. Figure 7 indicates that the tensile strength and the initial modulus of all para-position PSA fiber prepared in this article were 4.4 cN/dtex and 48 cN/dtex, respectively, whereas the tensile strength and the initial modulus of common PSA fibers were 2.4 cN/dtex and 35 cN/dtex, respectively. The tensile strength and the initial modulus of Nomex tested in this article were 5.4 cN/dtex and 83 cN/dtex, respectively, although the initial modulus of all para-position PSA fiber was still a little low, its tensile strength is approaching that of Nomex.

#### CONCLUSIONS

Although the presence of more rigid segments of *p*-phenylene in the PSA copolymer backbone did not increase the thermal stability of PSA fiber, it does enhance the strength and modulus of the fiber. The additional properties of PSA fibers, Nomex, and the prepared all para-position PSA fibers are listed in Table I.<sup>3,27,28</sup> As it can be seen from the table, all para-position PSA fiber shows better mechanical properties than the usual PSA fiber, and better thermal stability and flame-retardant properties than Nomex. We believe that all para-position PSA fiber will be widely used in various fields. The inherent viscosity of the polymer used in this article was still a little low, which indicated the low molecular weight of the polymer. It might be increased by a better synthesis process, and then the tensile strength of the all para-position PSA fiber might increase too. This article provided a simple and safe method for preparing the all para-position PSA fiber. LiCl acted as a cosolvent in the DMAc/LiCl system, some other cheaper and safer cosolvent like CaCl<sub>2</sub> or NH<sub>4</sub>Cl might be used in the future.

## REFERENCES

1. Ren, J. R.; Wang, X. F.; Zhang, Y. H. *Tech. Textiles* **2007**, *25*, 1.
2. Wang, X. F. Shanghai Textile Holding (Group) Co. CN. 1389604A, January **8**, **2003**.
3. Wang, X. F.; Zhang, Y. H. *China Textile Leader* **2005**, *1*, 18.
4. Zhang, L.; Li, Y. B.; Liu, J. Z. *J. Tianjin Polytechnic Univ.* **2006**, *25*, 17.
5. Wang, X. W.; Hu, Z. M.; Liu, Z. F. *Mater. Rev.* **2007**, *21*, 53.
6. Wu, H. Y.; Duan, Y. F. *Knitting Ind.* **2006**, *2*, 24.
7. Lu, X. R.; Gao, C. J.; Sun, X. Z. *Desalination* **1985**, *54*, 207.
8. Fan, G.; Zhang, C. J.; Zheng, L. Y. *Desalination* **1985**, *56*, 325.
9. Wang, S. S.; Ling, A. L.; Wu, L. L.; Gao, Y. Y.; Liu, S. X.; Wang, Z. Z.; Sheng, L. M.; Kang, D. K. *Desalination* **1987**, *62*, 221.
10. Sun, X. Z.; Zhang, M.; Lu, X. R.; Gao, C. J. *Desalination* **1987**, *62*, 353.
11. Jia, X. L.; Li, G.; Sui, G.; Li, P.; Yu, Y. H.; Liu, H. Y.; Yang, X. P. *Mater. Chem. Phys.* **2008**, *112*, 823.
12. Jia, X. L.; Li, G.; Yu, Y. H.; Sui, G.; Liu, H. Y.; Li, Y. N.; Li, P.; Yang, X. P. *J. Appl. Polym. Sci.* **2009**, *113*, 283.
13. Jia, X. L.; Yu, Y. H.; Li, G.; Sui, G.; Li, P.; Yang, X. P. *J. Appl. Polym. Sci.* **2010**, *118*, 1060.
14. Liu, L.; Wang, W. T.; Xiao, C. F. *J. Shanghai Jiaotong Univ. (Sci.)*, **2010**, *15*, 114.
15. Yu, J. L.; Yan, X.; Wang, X. F.; Feng, Y. P. In Proceedings of 2009 International Conference on Advanced Fibers and Polymer Materials, Shanghai, China, October 21–24, **2009**.
16. Qian, Y.; Huang, C. B.; Ding, Q. P.; Lai, C. L.; Chen, S. L.; Chen, F. *Polym. Mater. Sci. Eng.* **2006**, *22*, 42.
17. Wu, W. T. Relationship between spinning technology and structure–property of polyarylsulphonamide fiber. M.S. Thesis, University of Donghua, Shanghai, January **2010**.
18. Zhang, H. H.; Zhen, W.; Chen, Y. P. *Spectroscopy: Principles and Applications*; Chemical Industry Press: Beijing, **2011**; **Chapter 3**, pp 104.
19. Agrawal, A. K.; Jassal, M.; Sahoo, A.; Garapati, S. K. *J. Appl. Polym. Sci.* **2011**, *119*, 837.
20. Zhang, J.; Zhang, Y. W.; Zhao, J. X. *Polym. Bull.* **2011**, *67*, 1073.
21. Dong, R. J.; Zhao, J. X.; Zhang, Y. W.; Pan, D. *J. Polym. Sci. Part B: Polym. Phys.* **2009**, *47*, 261.
22. Dong, R. J.; Keuser, M.; Zeng, X. M.; Zhao, J. X.; Zhang, Y. W.; Wu, C. X.; Pan, D. *J. Polym. Sci. Part B: Polym. Phys.* **2008**, *46*, 1997.
23. Hermans, P. H.; Weidinger, A. *Die Makromol. Chem.* **1961**, *44*, 24.
24. Benedetti, A.; Cocco, G.; Fagherazzi, G.; Locardi, B.; Meriani, S. *J. Mater. Sci.* **1983**, *18*, 1039.
25. Zhang, M. Z.; Liu, B. J.; Gu, X. Y. *Research Method of Polymer*; China Light Industry Press: Beijing, **2000**; p 78.
26. Wong, K. K. H.; Zinke-Allmang, M.; Wan, W. *J. Mater. Sci.* **2010**, *45*, 2456.
27. Song, J. C. *Silk Textile Technol. Overseas* **2007**, *2*, 38.
28. García, J. M.; García, F. C.; Serna, F.; Peña, J. L. *Prog. Polym. Sci.* **2009**, *35*, 623.